ISBN: 978-3-95450-236-3 ISSN: 2673-7027 doi:10.18429/JACoW-eeFACT2022-WEYAT0101

COLLECTIVE EFFECTS STUDIES FOR CEPC

Na Wang[1†], Yuan Zhang[1, 2], Haisheng Xu[1], Saike Tian[1], Yudong Liu[1], Chuntao Lin[3]
[1]Institute of High Energy Physics, CAS, Beijing, 100049, China
[2] University of Chinese Academy of Sciences, CAS, Beijing, 100049, China
[3]Institute of Advanced Science Facilities, Shenzhen, China

Abstract

The impedance model of the Circular Electron Positron Collider (CEPC) storage ring is updated according to the development of the vacuum components based on the circular beam pipe. With the impedance model, the single bunch and coupled bunch instabilities for different operation scenarios are investigated. Particularly, the key instability issues driven by the beam coupling impedance in the Z operation mode are discussed. The influence of the longitudinal impedance on the transverse mode coupling instability is analysed both numerically and analytically. In addition, trapped ions can induce bunch centroid oscillation and emittance growth. The possibility of ion trapping and fast beam ion instability in the CEPC storage ring are also investigated.

INTRODUCTION

The Circular Electron Positron Collider (CEPC) is a double ring lepton collider covers a wide beam energy range from 45 GeV (Z-pole) to 180 GeV (tt-bar) [1,2]. Since the Z mode has the lowest beam energy, as well as highest beam current and slowest synchrotron radiation damping, normally it shows the most critical requirements on the collective effects. In order to estimate the influence of these effects, the impedance model of the CEPC collider has been evolving since the start of the project [3-6]. Based on the impedance, systematic studies on the beam instability issues and their mitigations have been performed. In this paper, the resistive wall impedance and its induced coupled bunch instability are updated by considering more detailed vacuum chamber designs. In addition, macro particle simulations are performed for the single bunch effect and beam ion instabilities. The perturbation of longitudinal impedance on the transverse mode coupling instability is investigated analytically.

IMPEDANCE MODELING

The impedance model is developed considering both resistive wall and geometrical impedances. The main vacuum chamber has a circular cross section with radius of 28 mm, which is made of copper and has a layer of NEG coating on its inner surface to reduce the secondary electron yield as well as for the vacuum pumping. In order to evaluate the resistive wall impedance, multi-layer analytical formula from field matching is used [7].

Meanwhile, simplified formulas are derived for longitudinal and transverse resistive wall impedance of the coated metallic chambers:

$$Z_{||}^{\mathrm{RW}}(\omega)=\frac{Z_0\delta_1\mu_1 k_0[\mathrm{sgn}(\omega)-i]}{4\pi b\mu_0}\times\frac{\alpha\tanh(x_1)+\tanh(x_2)}{\alpha+\tanh(x_1)\tanh(x_2)} \quad (1)$$

$$Z_{\perp}^{\mathrm{RW}}(\omega)=\frac{4-k_r^2b^2}{\sqrt{k_0^2+k_r^2}}\frac{1-i\mathrm{sgn}(\omega)}{4\pi b^3\delta_1\sigma_1}\times\frac{1+\alpha\tanh(x_1)\tanh(x_2)}{\alpha\tanh(x_2)+\tanh(x_1)} \quad (2)$$

where b is the beam pipe aperture, $\alpha=\delta_1\mu_1/\delta_2\mu_2$, $x_i=\lambda_i d_i$, $\lambda_i\simeq\sqrt{-2i}/\delta_i$, δ_i, d_i and μ_i are the skin depth, thickness and conductivity of the i'th layer, respectively. The numerical results are benchmarked with ImpedanceWake2D [8] and excellent agreements have been reached in the frequency range of interest.

Except the typical NEG coated vacuum chambers, the resistive wall impedance contributed by the MDI chambers, collimators in the interaction region and stainless steel chambers for flanges, bellows and BPMs are also considered. Since the Machine Detector Interface (MDI) and collimators may contribute large impedances, either due to the smaller beam pipe aperture or large local beta functions, the resistive wall impedance of the tapers are considered in more detail. Assuming the longitudinal and transverse resistive wall impedance is inverse proportional to the radius r or cubic of r, by integrating the impedance along the taper, we get the longitudinal and transverse resistive wall impedance of a taper is the impedance of a cylinder of unit length with the smaller aperture r_1 of the taper multiplied by the following factors

$$f_{||}^{RW}=\frac{r_1}{\tan\theta}\log\left(1+L/r_1\tan\theta\right), \quad (3)$$

$$f_{T}^{RW}=\frac{r_1}{2}\frac{2r_1/L+\tan\theta}{(r_1/L+\tan\theta)^2}, \quad (4)$$

where L and θ are the length and angle of the taper, respectively.

The longitudinal and transverse resistive wall impedance contributed from different vacuum components is summarized in Fig. 1 and Fig. 2, respectively. Here, the transverse impedance has been normalized by the local beta functions. In addition, geometrical form factors [9] are considered for the resistive wall impedance of the vacuum chambers with non-axial symmetry. We can see that the impedance contributed by the typical vacuum chamber dominates both the longitudinal and transverse resistive wall impedance. The contributions from the MDI and collimators are considerably small.

† wangn@ihep.ac.cn

ISBN: 978-3-95450-236-3 ISSN: 2673-7027 doi:10.18429/JACoW-eeFACT2022-WEYAT0101

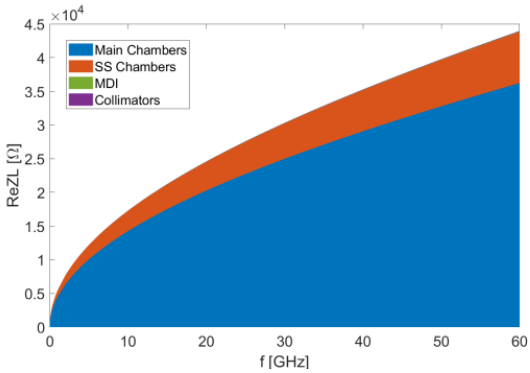

Figure 1: Real part of the longitudinal resistive wall impedance contributed from different type of vacuum chambers.

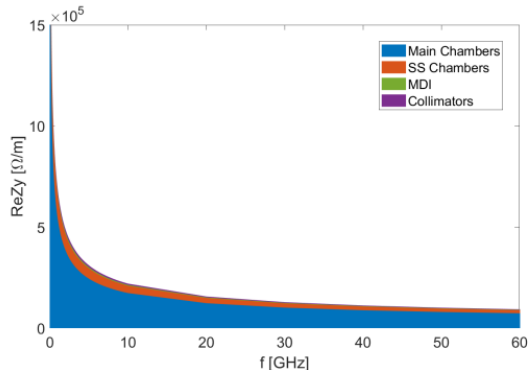

Figure 2: Real part of the transverse resistive wall impedance contributed from different type of vacuum chambers.

On the other hand, the geometrical impedances are simulated by CST [10] and ABCI [11] codes. The impedance generated by the RF cavities, flanges, bellows, gate valves, pumping ports, BPMs, collimators in the interaction region, and the electro separators, are included in the impedance model. Figures 2 and 3 show the total longitudinal and transverse impedances by summing up all the impedance contributors. The results show that both longitudinal and transverse broadband impedance are dominated by the resistive wall, flanges and bellows. Here, we should note that the impedance contributed by the injection and extraction elements, feedback kickers, absorbers, as well as masks and collimators outside the interaction region are not included yet. The impedance model will be continuously updated along with the development of the hardware designs.

The impedance budget calculated with an rms bunch length of 3mm gives the total longitudinal broadband impedance of 15.8 mΩ and transverse kick factor of 25.0 kV/pC/m. The results are more or less consistent with the CDR budget. The main difference is due to revision of the chamber cross section, more detailed number of elements, and more contributors included.

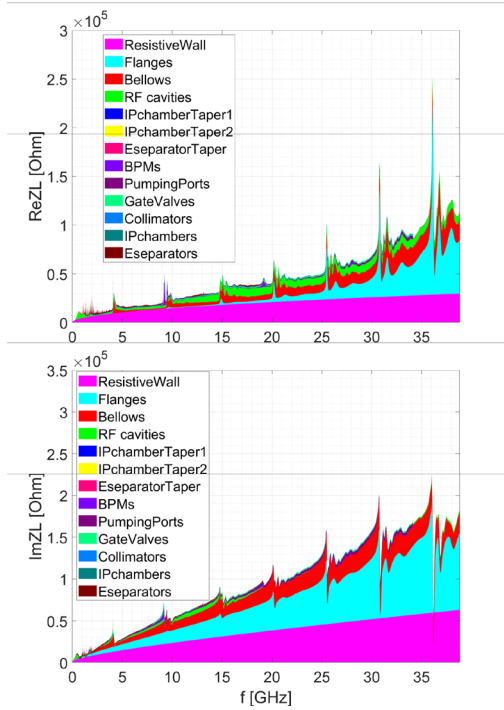

Figure 3: Real (top) and imaginary (bottom) part of the longitudinal impedance contributed from different vacuum components.

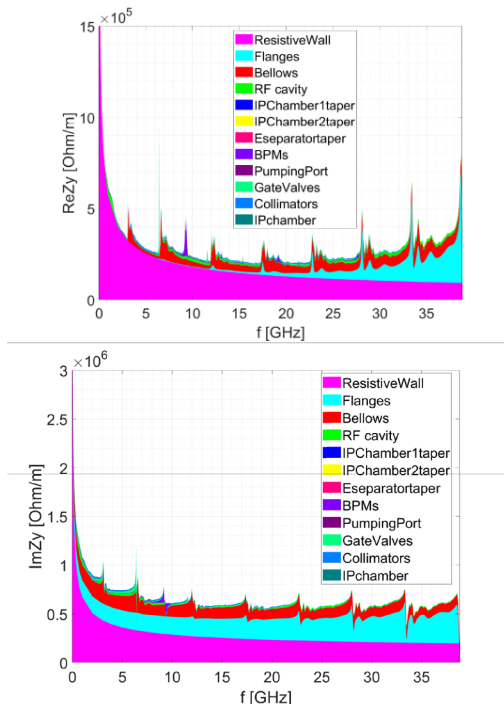

Figure 4: Real (top) and imaginary (bottom) part of the transverse impedance contributed from different vacuum components.

IMPEDANCE EFFECTS

Based on the impedance model, the collective effects are estimated by both analytical estimation and numerical simulations. Preliminary estimations on the instability

ISBN: 978-3-95450-236-3 ISSN: 2673-7027 doi:10.18429/JACoW-eeFACT2022-WEYAT0101

threshold for different operation scenarios are first given based on the analytical criterions. For the single bunch effect, the longitudinal impedance is above the threshold of Higgs, W and Z. This will induce bunch lengthening, energy spread increase, as well as synchrotron tune shift and spread. Although the criterion usually underestimates the instability threshold, we do observe its influence on the beam-beam interactions, which forced the optimization on the lattice design [12, 13]. In the transverse case, the impedance is above the threshold only for the Z operation mode, which will induce transverse mode coupling instability. This is a fast instability and normally with beam losses. For the multi-bunch case, there are also tight requirements on the narrowband impedance for Z. The thresholds on the narrowband impedance are at least two orders lower than the other energies. Therefore, the high order modes need to be well controlled to meet the requirements. In the following, the detailed analysis on instability issues driven by the impedance for Z will be discussed. The main beam parameters used in the following studies are listed in Table 1.

Table 1: Main beam parameters of CEPC Z

Parameter	Symbol	Value
Beam energy	E [GeV]	45.5
Circumference	C [km]	100
Beam current	I_0 [mA]	803.5
Bunch number	n_b	11934
Mom. compaction	α_p	1.43×10^{-5}
Betatron tune	ν_x/ν_y	317.1/317.22
Synchrotron tune	ν_s	0.035
Radiation damping	$\tau_x/\tau_y/\tau_z$ [ms]	850/850/425

Microwave Instability

In the longitudinal case, the threshold current of the microwave instability is approximately half of the design bunch intensity at 22.4 nC, as shown in Fig. 5. At the same time, we can also found apparent bunch lengthening and synchrotron tune shift and spread, even below the threshold, as shown in Figs. 5 and 6. The above effects will further influence the beam-beam interaction according to more consistent studies including both beam-beam and impedance [12, 13] due to the X-Z coupling [14]. On the other hand, we can expect additional bunch lengthening and energy spread increase due to the beamstrahlung, which will mitigate the perturbation induced by the impedance in the longitudinal plane.

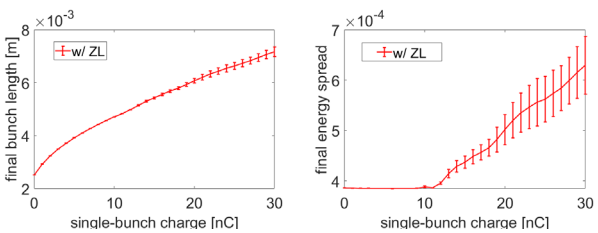

Figure 5: Variation of bunch length and incoherent synchrotron tune shift with bunch intensity.

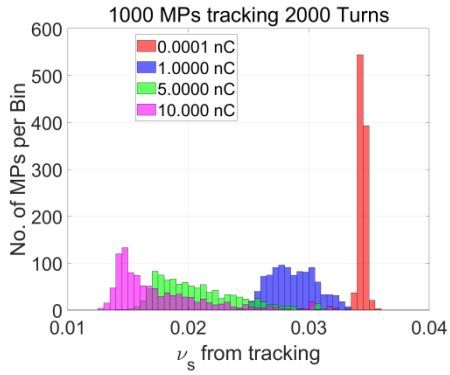

Figure 6: Histogram of the incoherent synchrotron tune at different bunch intensity.

Transverse Mode Coupling Instability

The transverse mode coupling instability is the main constraint on the single bunch current. The instability has been investigated in three different ways.

Analytical Estimations with Classical Vlasov Solver Mode analysis with and without impedance induced bunch lengthening are calculated. The results are shown in Fig. 7. Without bunch lengthening, the TMCI threshold is around 60% of the design value. When consider the impedance bunch lengthening, the analytical estimations show that threshold current will be increased by approximately a factor of two. The instability is supposed to be further detuned when consider bunch lengthening due to the beamstrahlung.

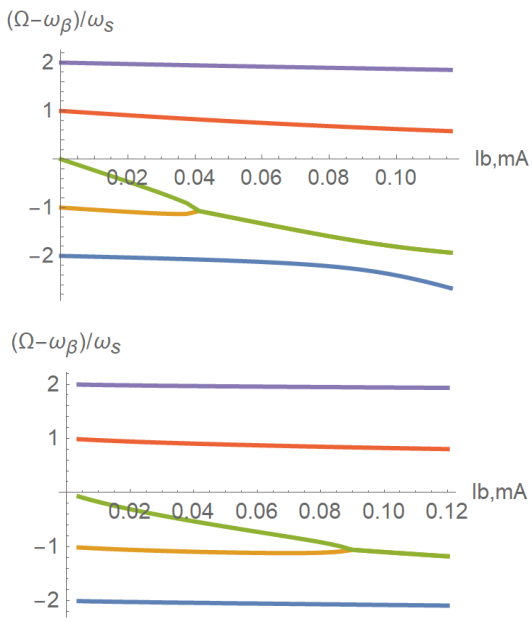

Figure 7: Dependence of the transverse mode frequency shift on the bunch current, without impedance induced bunch lengthening (up) and when the bunch lengthening at different bunch current been taken into account (bottom).

Micro particle simulations Particle tracking simulations including the longitudinal and transverse impedance

ISBN: 978-3-95450-236-3 ISSN: 2673-7027 doi:10.18429/JACoW-eeFACT2022-WEYAT0101

consistently are performed with the code Elegant [15]. The results are shown in Fig. 8, and compared with the case without longitudinal impedance. Without longitudinal impedance, the instability threshold is around 14 nC, which is consistent with the analytical estimation of the same case as given in Fig. 7. However, when include the longitudinal impedance, the instability gets more unstable and the threshold decreased to 10 nC, which is much lower than the analytical estimation only with bunch lengthening. Above the threshold, apparent beam losses and transverse centroid oscillations are observed. On the other hand, the shift of mode 0 below the threshold is still consistent with the analytical results. The instability is suspected to be induced by the enhanced mode coupling due to the smaller incoherent synchrotron tune. To mitigate the instability, dependence of the threshold beam current on the chromaticity is checked. The results show that the threshold current even decreases with increase of the chromaticity. Here, it should be noted that the nonlinear effects due to the variation of the transverse tune with amplitude is not included yet, which is expected to help in damping the instability.

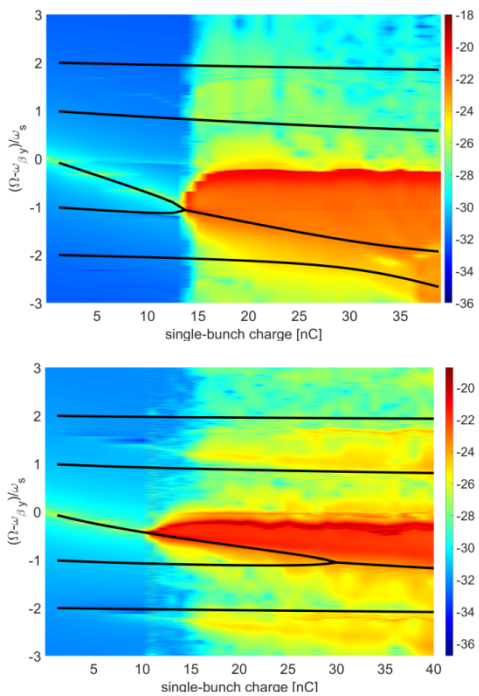

Figure 8: Variation of the transverse mode frequency shift with bunch intensity obtained from macro particle simulations, without (up) and with (bottom) longitudinal impedance. Different colour represents the amplitude of the FFT of the bunch centroid oscillation, and the black lines shows the analytical estimation on the mode frequency shift.

Analytical estimation considering the longitudinal perturbations Mode analysis considering perturbations from longitudinal impedance, as well as lengthened bunch from beamstrahlung, is performed using the method in Ref. [16]. Both longitudinal phase space distribution and synchrotron tune are projected into different action and angles. Considering the bunch lengthening from beamstrahlung, we get the instability threshold with longitudinal impedance as shown in Fig. 9. Including the longitudinal impedance, the higher order modes shift to mode 0 with wider bandwidth, and the instability threshold is decreased from 36 nC to 30 nC.

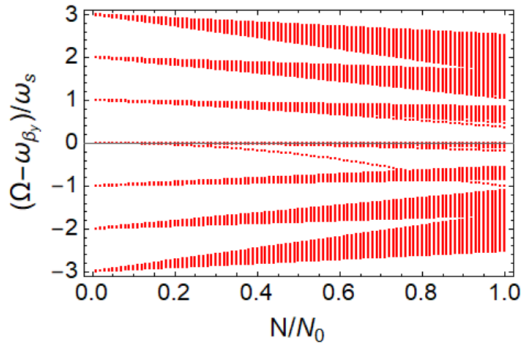

Figure 9: Variation of the transverse mode frequency shift with bunch intensity by considering the longitudinal impedance consistently.

Transverse Resistive Wall Instability

For the multi-bunch effects, coupled bunch instability driven by the resonance at zero frequency of the transverse resistive wall impedance gives extremely fast instability growth rate in the order of several turns. The transverse resistive wall impedance around zero frequency contributed by different vacuum components is shown in Fig. 10. The most dangerous mode is at frequency of –2.338 kHz, and the growth rate is dominated by the typical vacuum chamber. The instability is much faster than the synchrotron radiation damping and gives tough requirements on the feedback system. A combination of broadband feedback and mode feedback is proposed to damp the instability.

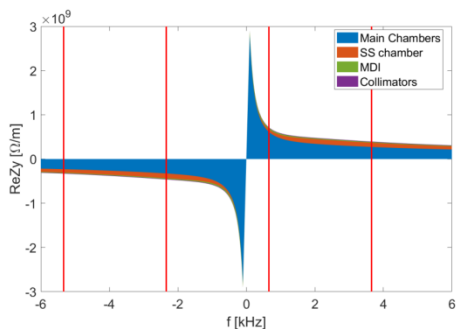

Figure 10: Transverse resistive wall impedance contributed by different type of vacuum chambers.

FAST BEAM ION INSTABILITY

Trapped ions can induce bunch centroid oscillation and emittance growth. The possible of ion trapping and fast beam ion instability are investigated. With vacuum pressure of 1 nTorr, and CO as the ion species, analytical estimations show that the instability growth for W and Z

ISBN: 978-3-95450-236-3 ISSN: 2673-7027 doi:10.18429/JACoW-eeFACT2022-WEYAT0101

are faster than synchrotron radiation damping, even considering multi bunch train filling pattern.

Particle tracking simulations are also performed with Elegant for different betatron functions. Multi-train filling pattern is effective in mitigating the beam ion instability. However, except the case with very low betatron functions at the interaction point, both horizontal and veritcal beam centroid oscillation amplitude increased to larger than 10% of the transverse beam size, and then saturate at around the scale of the beam size. Beam emittance growth is also foreseen. One example with ring average betatron functions is shown in Fig 11. Therefore, bunch by bunch feedback is needed to damp the instability.

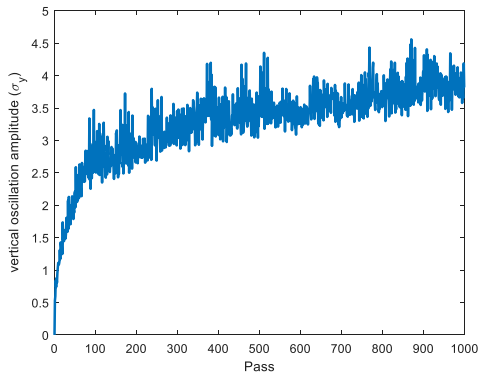

Figure 11: Variation of the vertical bunch centroid oscillation with number of turns under the influence of ions.

CONCLUSION

The collective beam instabilities are potential restrictions in CEPC to achieve high luminosity performance. Systematic studies have been performed to investigate the influence from the collective effects. The results show no apparent showstoppers from collective effects for the high energy operation modes, except for Z. The main constraint for the single bunch current is from the transverse mode coupling instability. The instability threshold is below the design current when including both longitudinal and transverse impedance consistently. The possible mitigations are investigated. The total beam current is mainly constraint by the transverse resistive wall instability, which gives tough requirements on the bunch-by-bunch feedback designs. In addition, the beam ion effects also show influence on the beam stability even considering a multi-train filling pattern, and feedback is required. Besides, consistent studies also show crosstalk between the transverse impedance and the beam-beam interaction. Therefore, collective effects studies need to get more involved with beam-beam and hardware designs.

REFERENCES

[1] CEPC Study Group, "CEPC Conceptual Design Report: Volume 1 – Accelerator," arXiv:1809.00285 [physics.acc-ph], 2018. doi:10.48550/arXiv.1809.00285

[2] Y.W. Wang *et al*., "Lattice design of the CEPC collider ring for a high luminosity scheme", in *Proc. IPAC'21*, Campinas, Brazil, May 2021, pp. 2679-2682. doi:10.18429/JACoW-IPAC2021-WEPAB033

[3] N. Wang *et al*, "Impedance and collective effects studies in CEPC", in *Proc. HF'14*, Beijing, China, Oct. 2014, paper SAT4B1, pp. 218-222.

[4] N. Wang *et al.*, "Instability issues in CEPC", in *Proc. eeFACT'16*, Daresbury, UK, Oct. 2016, pp. 108-111. doi:10.18429/JACoW-eeFACT2016-TUT3AH2.

[5] N. Wang, Y. D. Liu, H.J. Zheng, D.J. Gong and J. He, "Collective effects in CEPC", in *ICFA Beam Dynamics Newsletter* no. 72, p. 55, 2017.

[6] Na Wang *et al.*, "Mitigation of Coherent Beam Instabilities in CEPC", in *Proc. of ICFA mini-Workshop on Mitigation of Coherent Beam Instabilities in Particle Accelerators* (MCBI 2019), Zermatt, Switzerland, Sep. 2019, CERN-2020-009 (2020), p. 286. doi:10.23732/CYRCP-2020-009.286.

[7] N. Wang and Q. Qin, "Resistive-wall impedance of two-layer tube", *Phys. Rev. Spec. Top. Accel Beams*, vol. 10, 111003, 2007. doi:10.1103/PhysRevSTAB.10.111003

[8] N. Mounet, "The LHC Transverse Coupled-Bunch Instability (Ph.D. thesis)", Ecole Polytechnique, Lausanne, 2012.

[9] Y.T. Wang, N. Wang, H.S. Xu and G. Xu, "Tune shift due to the quadrupolar resistive-wall impedance of an elliptical beam pipe", *Nucl. Instrum. Methods Phys. Res., Sect. A*, vol. 1029, p. 166414, 2022. doi:10.1016/j.nima.2022.166414

[10] CST Particle Studio, http://www.3ds.com.

[11] Yong Ho Chin, http://abci.kek.jp/abci.htm.

[12] Y. Zhang *et al.*, "Self-consistent simulations of beam-beam interaction in future e^+e^- circular colliders including beamstrahlung and longitudinal coupling impedance", *Phys. Rev. Spec. Top. Accel Beams*, vol. 23, p. 104402, 2020. doi:10.1103/PhysRevAccelBeams.23.104402

[13] C. Lin, K. Ohmi, and Y. Zhang, "Coupling effects of beam-beam interaction and longitudinal impedance", *Phys. Rev. Accel. Beams*, vol. 25, p. 011001, 2022. doi:10.1103/PhysRevAccelBeams.25.011001

[14] K. Ohmi, N. Kuroo, K. Oide, D. Zhou, and F. Zimmermann, "Coherent Beam-Beam Instability in Collisions with a Large Crossing Angle", *Phys. Rev. Lett.*, vol. 119, p. 134801, 2017. doi:10.1103/PhysRevLett.119.134801

[15] M. Borland, "elegant: A Flexible SDDS-Compliant Code for Accelerator Simulation", Advanced Photon Source LS-287, 2000.

[16] Y. Wang and M. Borland, "Pelegant: A Parallel Accelerator Simulation Code for Electron Generation and Tracking", in *Proc. of the 12th Advanced Accelerator Concepts Workshop*, AIP Conf. Proc., vol. 877, p. 241, 2006.